Original Article

J Korean Soc Radiol 2023;84(6):1309-1323
https://doi.org/10.3348/jksr.2023.0008
eISSN 2951-0805

JOURNAL of THE KOREAN SOCIETY of RADIOLOGY

Impact of Deep-Learning Based Reconstruction on Single-Breath-Hold, Single-Shot Fast Spin-Echo in MR Enterography for Crohn's Disease

크론병에서 자기공명영상 장운동기록의 단일호흡 단발 고속 스핀 에코기법: 딥러닝 기반 재구성의 영향

Received January 20, 2023
Revised March 18, 2023
Accepted May 6, 2023

***Corresponding author**
Yedaun Lee, MD,
Department of Radiology,
Inje University College of Medicine,
Haeundae Paik Hospital,
875 Haeun-daero, Haeundae-gu,
Busan 48108, Korea.

Tel 82-51-797-0355
Fax 82-51-797-0379
E-mail chosai81@gmail.com

This is an Open Access article distributed under the terms of the Creative Commons Attribution Non-Commercial License (https://creativecommons.org/licenses/by-nc/4.0) which permits unrestricted non-commercial use, distribution, and reproduction in any medium, provided the original work is properly cited.

Eun Joo Park, MD[1], Yedaun Lee, MD[1*], Joonsung Lee, PhD[2]

[1]Department of Radiology, Inje University College of Medicine, Haeundae Paik Hospital, Busan, Korea
[2]GE Healthcare Korea, Seoul, Korea

ORCID iDs
Eun Joo Park https://orcid.org/0000-0003-2450-9365,
Yedaun Lee https://orcid.org/0000-0002-9801-8449,
Joonsung Lee https://orcid.org/0000-0002-0164-1139

Purpose To assess the quality of four images obtained using single-breath-hold (SBH), single-shot fast spin-echo (SSFSE) and multiple-breath-hold (MBH) SSFSE with and without deep-learning based reconstruction (DLR) in patients with Crohn's disease.

Materials and Methods This study included 61 patients who underwent MR enterography (MRE) for Crohn's disease. The following images were compared: SBH-SSFSE with (SBH-DLR) and without (SBH-conventional reconstruction [CR]) DLR and MBH-SSFSE with (MBH-DLR) and without (MBH-CR) DLR. Two radiologists independently reviewed the overall image quality, artifacts, sharpness, and motion-related signal loss using a 5-point scale. Three inflammatory parameters were evaluated in the ileum, the terminal ileum, and the colon. Moreover, the presence of a spatial misalignment was evaluated. Signal-to-noise ratio (SNR) was calculated at two locations for each sequence.

Results DLR significantly improved the image quality, artifacts, and sharpness of the SBH images. No significant differences in scores between MBH-CR and SBH-DLR were detected. SBH-DLR had the highest SNR ($p < 0.001$). The inter-reader agreement for inflammatory parameters was good to excellent ($\kappa = 0.76–0.95$) and the inter-sequence agreement was nearly perfect ($\kappa = 0.92–0.94$). Misalignment artifacts were observed more frequently in the MBH images than in the SBH images ($p < 0.001$).

Conclusion SBH-DLR demonstrated equivalent quality and performance compared to MBH-CR. Fur-

Copyrights © 2023 The Korean Society of Radiology

JOURNAL of
THE KOREAN SOCIETY of
RADIOLOGY

thermore, it can be acquired in less than half the time, without multiple BHs and reduce slice misalignments.

Index terms Crohn's Disease; Magnetic Resonance Imaging; T2-Weighted-Imaging; Deep Learning Reconstruction

INTRODUCTION

MR enterography (MRE) is commonly performed in patients with Crohn's disease as it helps in diagnosing and monitoring their therapeutic response. Owing to the lack of ionizing radiation exposure, MRE has an advantage over CT in observing inflammation over a long period of time, particularly in young patients. In addition, MRE provides information acquired from multiple sequences, enabling the evaluation of the degree of inflammation using various features. Among these sequences, T2-weighted imaging is essential because it provides information on bowel wall thickening, bowel wall signal intensity, perienteric edema, and fluid collection, which are important features in determining the severity and extent of inflammation (1-4).

Fast image acquisition is mandatory to reduce the motion artifacts caused by bowel peristalsis and respiration. These motion artifacts result in image blurring, ghosting, signal loss, and the misalignment of slices, which may obscure the anatomical details or complicate bowel tracing (5), decreasing the diagnostic confidence. Single-shot fast spin-echo (SSFSE) is the most motion-robust T2-weighted acquisition technique; thus, it is preferred in performing MRE (6, 7). SSFSE is usually obtained by split acquisition over multiple-breath-holds (MBHs) for an adequate spatial resolution and coverage. However, the breath-holding positions may vary, resulting in a spatial mismatch in the acquired sections (8, 9). Moreover, repeated BHs can easily exhaust patients and reduce compliance. Therefore, single-BH (SBH) acquisition might have an advantage over MBH acquisition, such that it minimizes the misalignment and gross bowel motion between the BHs and shortens the scan time. With the application of a variable refocusing flip angle (VFA), image acquisition within an SBH has become possible while providing clinically acceptable T2 contrast (10). However, suboptimal image quality due to potential artifacts and a low signal-to-noise ratio (SNR) may hinder the substitution of standard-of-care images with those obtained from faster acquisitions (9, 11, 12).

A commercially available deep-learning based reconstruction (DLR) pipeline overcomes the tradeoff between the scan time and image quality. This technique addresses the fundamental image quality limitations of conventional reconstruction (CR) to provide images with a higher effective spatial resolution and less noise (13). We hypothesized that using DLR in SBH-SSFSE would be comparable to conventional MBH-SSFSE in MRE. Therefore, this study aims to compare SBH-SSFSE and MBH-SSFSE with and without DLR according to image quality and to evaluate the inter-sequence agreement for the findings that suggest the presence of active inflammation.

JOURNAL of THE KOREAN SOCIETY of RADIOLOGY

MATERIALS AND METHODS

PATIENT

This study was approved by the Institutional Review Board, and the requirement for an informed consent was waived because of its retrospective nature (IRB No. 2022-05-053).

Patients with known or suspected Crohn's disease, who underwent MRE between December 2020 and February 2022, were enrolled after we searched our institution's electronic medical database. Of the 86 patients who were initially identified, 25 with incomplete T2-weighted images in the workstation (i.e., not including either originally acquired T2-weighted SBH-SSFSE DLR or MBH-SSFSE DLR sequences) were excluded. Therefore, 61 patients (42 males and 19 females; mean age: 32.9 ± 1.5 [standard deviation {SD}] years) were included in the final analysis. Of the 61 patients, one underwent ileal loop resection, two underwent right hemicolectomy, and three underwent terminal ileal resection. Therefore, 60 segments of the ileal loop, 56 segments of the terminal ileum, and 59 segments of the ascending colon were evaluated for the severity of inflammation.

MRE ACQUISITION

MRE was performed using a 3T MRI scanner (SIGNA™ Architect, GE Healthcare, Waukesha, WI, USA) with two 30-channel coils (AIR™ anterior array coil, GE Healthcare). Before MRI acquisition, the patients ingested 1 L of polyethylene glycol solution (Coolprep, Taejoon Pharm, Seoul, South Korea) to achieve adequate bowel lumen distension. Coronal SSFSE T2-weighted images without fat saturation were acquired using SBH and MBH schemes, respectively. The SBH sequence was acquired with a VFA applied, while the MBH sequence was obtained at an initial FA of 155° and a fixed refocusing FA of 130°. The detailed imaging parameters are listed in Table 1.

Table 1. Imaging Scan Parameters

	Multiple-Breath-Hold SSFSE	Single-Breath-Hold SSFSE
Refocusing flip angles, °	Initial 155°, constant 130°	Initial 130°, minimum 90°, central 100°, last 45°
Bandwidth, Hz/pixel	90.91	111.11
Matrix	400 × 320	320 × 192
Field of view	380 × 380	380 × 380
No. of slice acquired	36	36
Slice thickness, mm	4	4
Slice gap, mm	0.4	0.4
Acceleration factor	2.00	3.00
Number of excitation	1.0	1.0
Echo time, msec	80	100
Repetition time, msec	1287.9	331.4
Scan time, sec, mean ± SD	53.19 ± 3.16	16.29 ± 0.99

SD = standard deviation, SSFSE = single shot fast spin echo

DLR

The commercially available DLR pipeline (AIR™ Recon DL, GE Healthcare) (14) was used to reconstruct images in the SBH and MBH sequences. The DLR was designed to reduce truncation artifacts, increase sharpness, and offer tunable noise reduction levels. A reduction factor of 75% (DL High) was selected for this study.

IMAGE ANALYSIS

Two blinded radiologists (with 2 and 12 years of subspecialty experience) independently reviewed the four image sets: MBH-DLR, MBH-CR, SBH-DLR, and SBH-CR. The subjective overall image quality was assessed using a 5-point Likert scale (1 = very poor quality, non-diagnostic; 2 = poor quality, significantly impaired diagnostic quality; 3 = fair quality, slightly impaired diagnostic quality; 4 = good quality; and 5 = excellent quality).

The overall image artifacts, synthetic appearance, and motion-related signal loss were scored using a 5-point scoring system. Similarly, higher scores (closer to 5) indicated fewer artifacts and better quality (15). Moreover, the sharpness of the bowel wall and vasa recta was evaluated using a 5-point scale; a score of 5 indicated a very clear and sharp visualization of the structures (16). The spatial misalignment of slices was evaluated not only using coronal images but also using reconstructed axial and sagittal images. One reader (with 2 years of subspecialty experience) reviewed the MBH and SBH images for the presence of a misalignment.

Mural thickness, mural signal intensity, and perimural signal intensity were scored using a 4-point scale in the ileum (excluding the terminal ileum), terminal ileum, and ascending colon, respectively, to evaluate the severity of inflammation (Table 2) (17). Readers were blinded to the endoscopic results.

The SNR was calculated at the level of the superior mesenteric artery (SMA) and iliac bifurcation. It was calculated by dividing the mean signal of the image slice by the estimated SD of the noise level, which was estimated using a hybrid discrete wavelet transform and an edge information removal-based algorithm (18). The conventional method to calculate the SNR using the SD of noise in the background air was not used because the imaging field-of-view was tightly selected and did not include much of the background air region. In addition, the background noise is non-homogenous on applying multichannel coils and parallel imag-

Table 2. MR Enterography Scoring System for Bowel Inflammation Severity

Parameter	Scoring			
	0	1	2	3
Bowel wall thickness, mm	1–3	> 3–5	> 5–7	> 7
Mural SI on T2 weighted image	Equivalent to that of normal bowel wall	Minor increase in SI	Moderate increase in SI	Marked increase in SI: bowel wall contains areas of high SI, approaching that of the luminal content
Perimural SI on T2 weighted images	Equivalent to that of normal mesentery	Increase in mesenteric SI but no fluid collection	Small fluid rim (≤ 2 mm)	Large fluid rim (> 2 mm)

SI = signal intensity

ing (19), and the SD calculation of the noise depends heavily on the location of the region of interest (ROI). Indeed, the multiple disease locations and the thinness of the bowel wall could confound the measurement of the ROI in the inflamed bowel walls caused by Crohn's disease. Other methods, such as structural similarity, which is used to calculate image quality from the ground-truth image, were not used as there was no ground-truth image in this study.

STATISTICAL ANALYSIS

The mean scores for the overall image quality, artifacts, image sharpness, synthetic appearance, and SNR of the four image sets were compared using the Friedman test. A Bonferroni correction was applied in multiple comparisons. The inter-reader and inter-sequence agreement of the mural thickness, mural signal intensity, and perimural signal intensity were calculated using the Cohen's kappa coefficient (κ). The kappa estimate was interpreted as poor agreement for a κ of < 0.20, fair for a κ = 0.21–0.40, moderate for a κ = 0.41–0.60, good for a κ = 0.61–0.80, and excellent for a κ = 0.81–1.00. The spatial misalignment artifacts were compared using the paired *t*-test. All the statistical analyses were performed using the SPSS version 28 (IBM Corp., Armonk, NY, USA).

RESULTS

ASSESSMENT OF VISUAL SCORING

The average score of the overall image quality was the highest in the MBH-DLR images (mean ± SD: 4.36 ± 0.45) compared with that of the other three sets. The SBH-CR images (3.10 ± 0.28) showed the lowest score. No significant difference was detected between the MBH-CR and SBH-DLR images (4.00 ± 0.18 and 3.98 ± 0.41, respectively, $p > 0.999$) (Fig. 1).

The overall artifact in the SBH-CR images (3.32 ± 0.47) was the most severe compared with that in the others ($p < 0.001$). No significant difference among the other three sets was detected. The most frequently visible artifacts were fine linear structures that appeared in the entire image, particularly in the SBH images. Moreover, artifacts caused by bowel peristalsis or respiratory motion were included.

Regarding the synthetic appearance, both DLR images scored lower than the corresponding conventional images ($p < 0.001$). No significant difference was found among the DLR images ($p > 0.999$).

The SBH images (4.11 ± 0.66 for SBH-CR) showed a significant ($p < 0.001$) motion-related signal loss compared with that in the MBH images (4.72 ± 0.45 for MBH-CR). No significant difference between the DLR images and the conventional images was observed.

The spatial misalignment artifacts were observed in the MBH images of 32 patients (52%) and in the SBH images of two patients (3.3%). The rates were higher in the MBH images than in the SBH images ($p < 0.001$) (Fig. 2).

The bowel wall sharpness was the clearest in the MBH-DLR images (4.34 ± 0.45) followed by that in the MBH-CR (4.04 ± 0.19) and SBH-DLR (3.95 ± 0.41) images. However, the differences were not statistically significant. The vasa recta sharpness was the highest in the SBH-DLR images (4.11 ± 0.39), followed by that in the MBH images. Both the bowel wall and vasa recta sharpness were the lowest in the SBH-CR images compared with those in the other sets

Fig. 1. Coronal single-shot fast spin-echo T2WIs of a 31-year-old male patient with Crohn's disease.
A-D. MBH T2WI with DLR (A), MBH T2WI with CR (B), SBH T2WI (C) with DLR, and SBH with CR (D). The DLR images show reduced background noise and higher sharpness of bowel margins and mesenteric vessels, compared with those in the corresponding CR images, and the SBH-DLR image shows a comparable image quality to that of the MBH images.
CR = conventional reconstruction, DLR = deep-learning based reconstruction, MBH = multiple-breath-hold, SBH = single-breath-hold, WI = weighted image

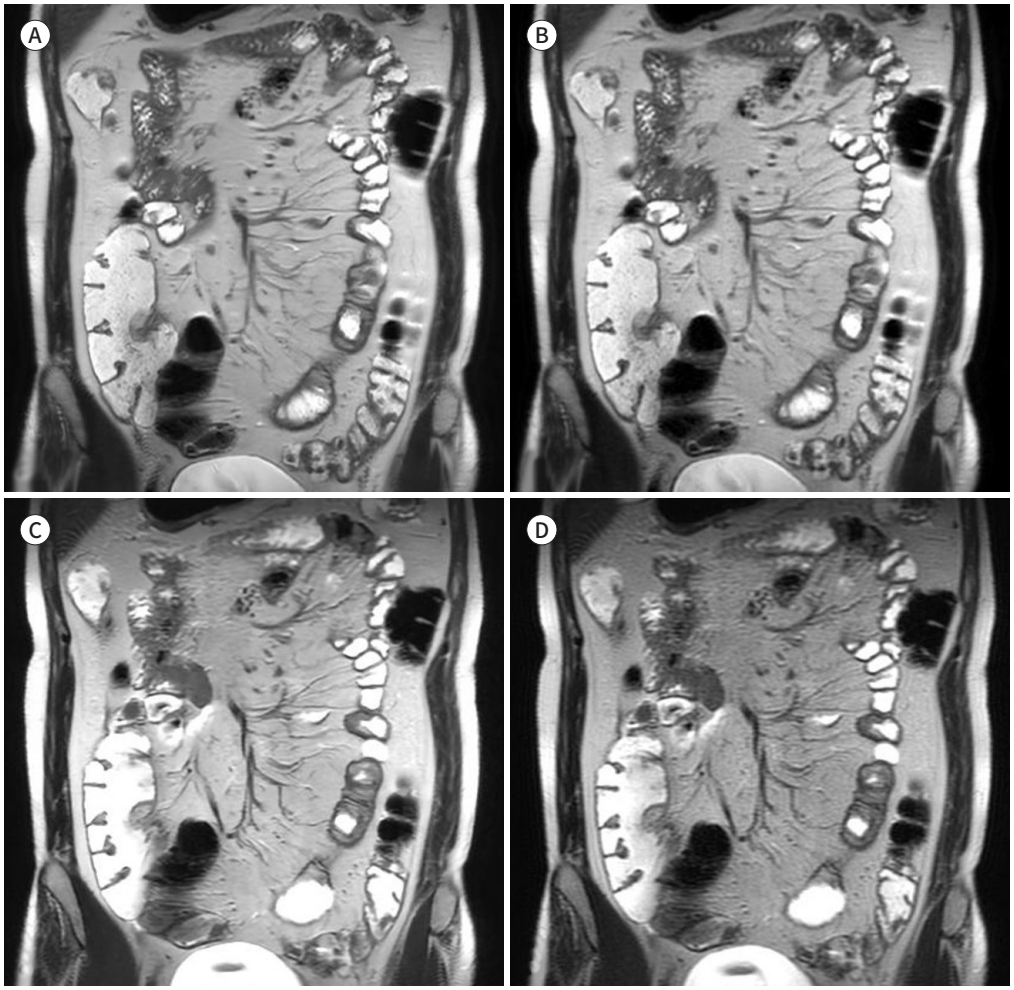

($p < 0.001$). The image quality scores are summarized in Table 3.

INFLAMMATORY LESION ANALYSIS

On lesion evaluation, the overall inter-reader agreement was good to excellent (κ value: 0.76–0.95). The inter-sequence agreement by both readers was excellent for all bowel segments (κ value: 0.94–1.00 by reader 1; 0.92–1.00 by reader 2) (Figs. 3, 4). The results are presented in Tables 4 and 5.

SNR

The highest SNR was detected in the SBH-DLR images at both the SMA and aortic bifurcation levels (mean ± SD: 135.32 ± 23.81 at the SMA level and 131.52 ± 23.9 at the aortic bifur-

cation level), followed by that in the MBH-DLR images (126.05 ± 19.94 at the SMA level and 126.99 ± 16.66 at the aortic bifurcation level), with no significant difference ($p > 0.999$). The DLR images showed a significantly higher SNR than that of the CR images for both the SBH

Fig. 2. Axial reconstruction images of a 22-year-old male patient (A, B) and a 47-year-old male patient (C, D) with Crohn's disease. Multiple-breath-hold-DLR images (A, C) and SBH-DLR images (B, D).
A, C. A slice misalignment appears as an inappropriately cut-off liver surface and abdominal wall muscles (arrows) because of the altered breath-holding position.
B, D. The reconstructed corresponding SBH images show continuous anatomical structures without any gap or skipped areas.
DLR = deep-learning based reconstruction, SBH = single-breath-hold

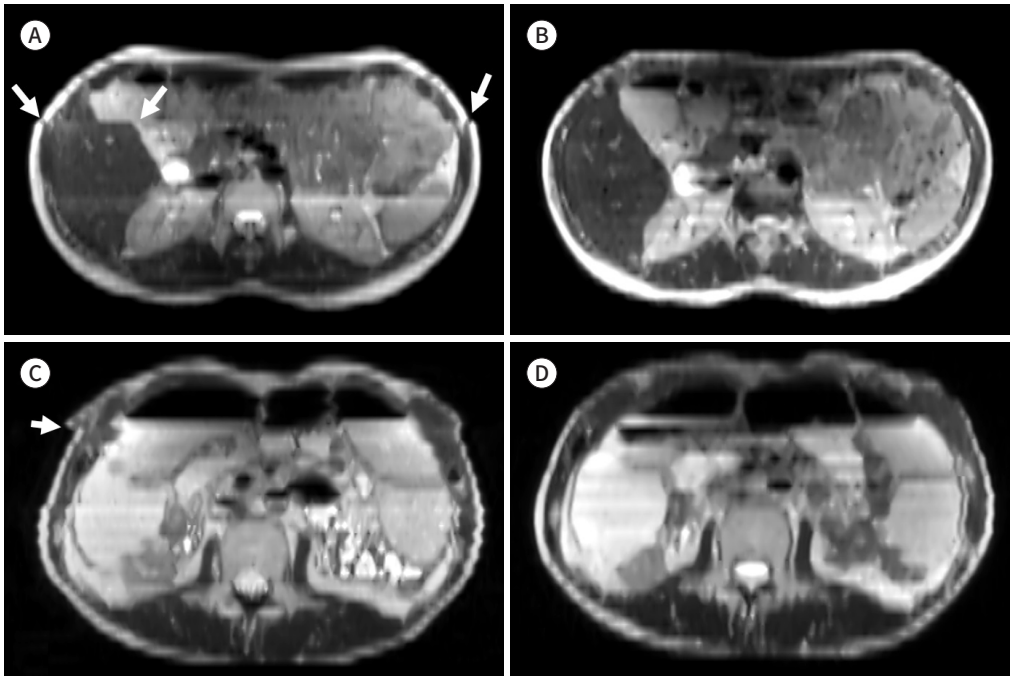

Table 3. Qualitative Analysis of Image Quality Scoring

Parameter	Image				*p*-Value
	MBH-DLR	MBH-CR	SBH-DLR	SBH-CR	
Overall image quality	4.36 ± 0.45 (4.0–5.0)	4.00 ± 0.18 (3.0–4.5)	3.98 ± 0.41 (3.0–5.0)	3.10 ± 0.28 (2.5–4.0)	< 0.001*
Overall artifacts	3.98 ± 0.44 (3.0–5.0)	3.84 ± 0.41 (3.0–4.5)	3.92 ± 0.34 (3.0–5.0)	3.32 ± 0.47 (2.5–4.0)	< 0.001†
Motion related signal loss	4.72 ± 0.45 (3.5–5.0)	4.72 ± 0.45 (3.5–5.0)	4.11 ± 0.65 (2.0–5.0)	4.11 ± 0.66 (2.0–5.0)	< 0.001‡
Bowel wall sharpness	4.34 ± 0.45 (4.0–5.0)	4.04 ± 0.19 (4.0–5.0)	3.95 ± 0.41 (3.0–5.0)	3.12 ± 0.31 (3.0–4.0)	< 0.001†
Vasa recta sharpness	4.05 ± 0.28 (3.5–5.0)	3.83 ± 0.31 (3.0–4.0)	4.11 ± 0.39 (3.0–5.0)	3.12 ± 0.34 (2.5–4.0)	< 0.001†
Synthetic appearance	3.98 ± 0.45 (3.0–5.0)	4.81 ± 0.33 (4.0–5.0)	4.32 ± 0.43 (3.5–5.0)	4.96 ± 0.17 (4.0–5.0)	< 0.001§

Data are presented as mean ± standard deviation (range). The score of 5 is the highest quality and has the least amount of artifact.
*The post hoc analysis showed significant difference between MBH-DLR and other three images. Also SBH-CR showed significant difference from MBH images and SBH-DLR. The MBH-CR and SBH-DLR showed no significant difference.
†The post hoc analysis demonstrated significant difference between SBH-CR and other three images. The MBH-DLR, MBH-CR, and SBH-DLR showed no significant difference.
‡The MBH and SBH images showed significant differences, regardless of reconstruction methods. The DLR and CR images showed no significant difference.
§The DLR images showed significant difference compared with corresponding CR images.
CR = conventional reconstruction, DLR = deep-learning based reconstruction, MBH = multiple-breath-hold, SBH = single-breath-hold

JOURNAL of
THE KOREAN SOCIETY of
RADIOLOGY

Fig. 3. Coronal SSFSE T2-weighted images of a 30-year-old male patient with Crohn's disease.
A-D. MBH-DLR (A), MBH-CR (B), SBH-DLR (C), and SBH-CR (D), respectively. The DLR images (A, C) show reduced noise with sharper margin of bowel wall compared with those in the CR images (B, D); better delineation of the bowel wall and of the inflammation (asterisks) in the cecum and terminal ileum with an enteroenteric fistula (arrows) and an enterocolic fistula (arrowheads); moreover, both readers gave all the four sequences the same scores regarding mural thickness, mural signal intensity, and perimural signal intensity.
E, F. Contrast-enhanced T1-weighted image (E) and diffusion restriction image (F) (b = 900) of the corresponding area. Contrast enhanced image show mural hyper-enhancement and wall thickening of cecum and terminal ileum (asterisks), enteroenteric fistula (arrows) and enterocolic fistula (arrowheads) which show diffusion restriction, suggesting active inflammation.
CR = conventional reconstruction, DLR = deep-learning based reconstruction, MBH = multiple-breath-hold, SBH = single-breath-hold

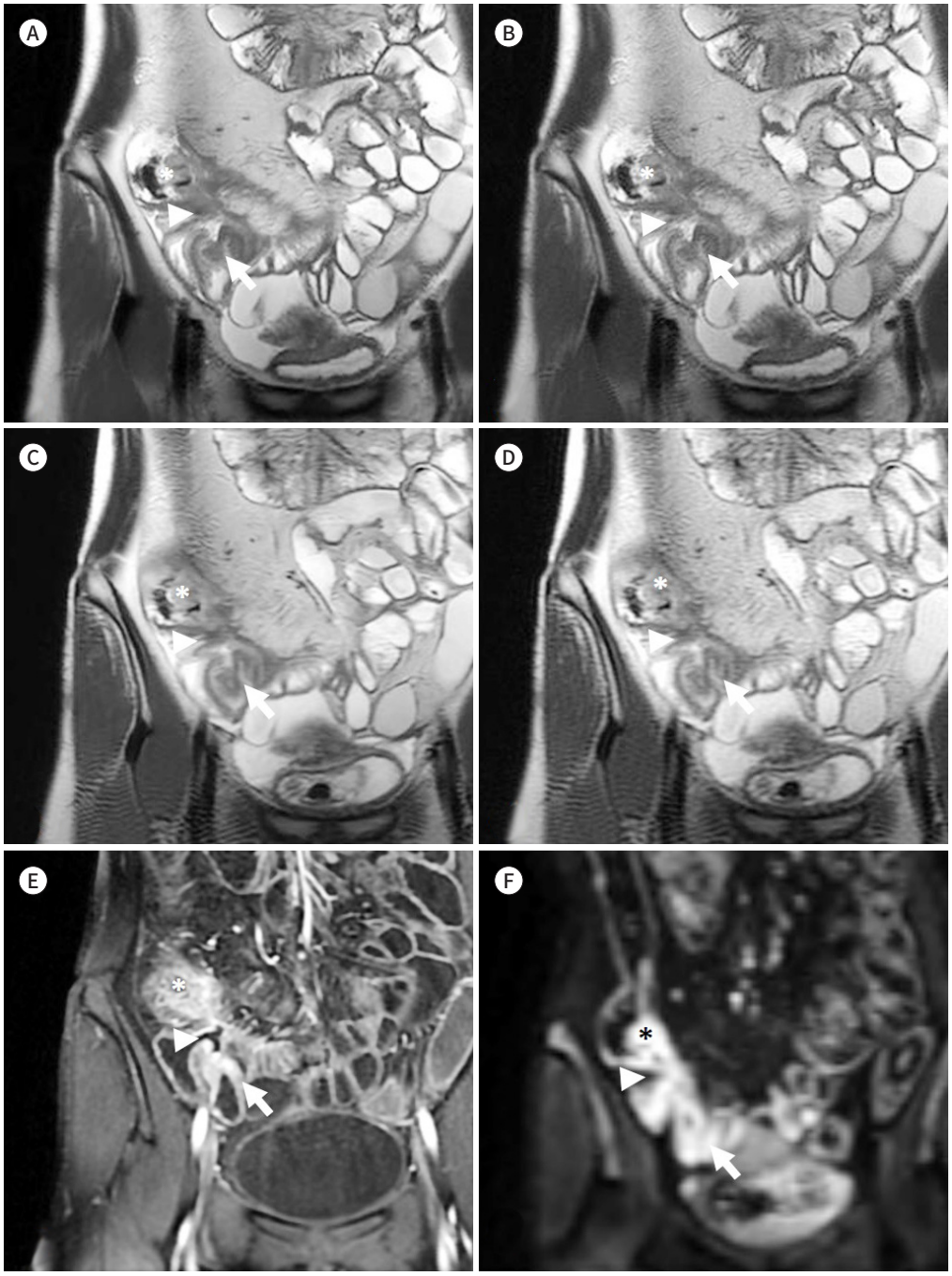

Fig. 4. Coronal SSFSE T2-weighted images of a 22-year-old female patient with Crohn's disease.
A-D. MBH-DLR (A), MBH-CR (B), SBH-DLR (C), and SBH-CR (D), respectively. Two readers gave all four images the same scores regarding the inflammatory parameters (e.g., mural thickness, mural signal intensity, and perimural signal intensity). Images show increased mural thickness and mural signal intensity (arrows), suggesting active inflammation.
E, F. Contrast-enhanced T1-weighted image (E) and diffusion restriction image (F) (b = 900) of the corresponding area show mural hyper-enhancement with diffusion restriction (arrows).
CR = conventional reconstruction, DLR = deep-learning based reconstruction, MBH = multiple-breath-hold, SBH = single-breath-hold

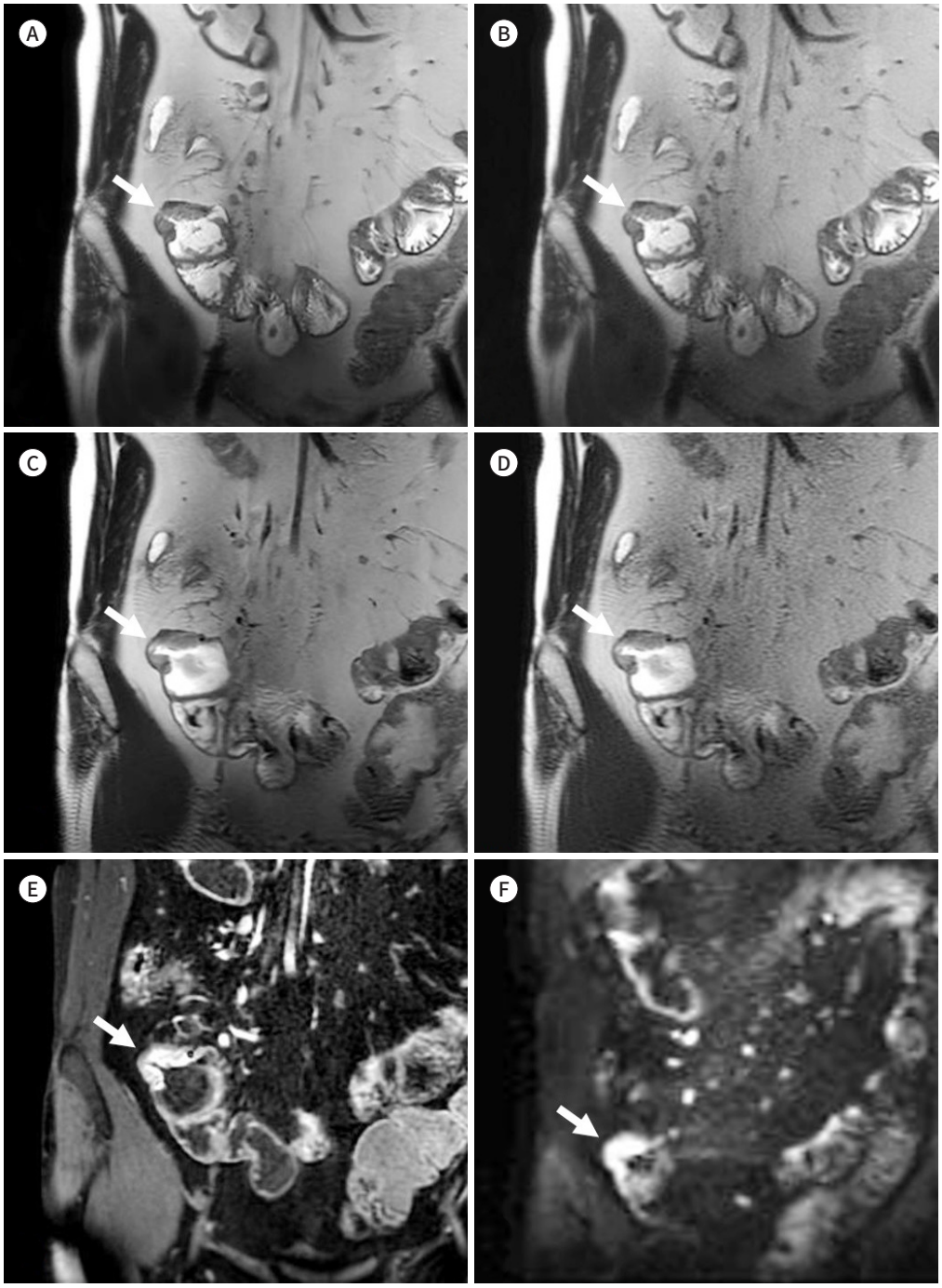

Table 4. Inter-Reader Agreement on Inflammatory Lesions

Parameter	Image			
	MBH-DLR	MBH-CR	SBH-DLR	SBH-CR
Ileum				
Mural thickness	0.91 (0.83-1.00)	0.91 (0.83-1.00)	0.91 (0.84-1.00)	0.88 (0.82-1.00)
Mural signal intensity	0.87 (0.84-1.00)	0.87 (0.84-1.00)	0.87 (0.84-0.99)	0.87 (0.84-0.99)
Perimural signal intensity	0.89 (0.78-1.00)	0.89 (0.78-1.00)	0.89 (0.78-1.00)	0.89 (0.78-1.00)
Terminal ileum				
Mural thickness	0.79 (0.81-0.96)	0.79 (0.81-0.96)	0.77 (0.79-0.95)	0.77 (0.79-0.95)
Mural signal intensity	0.76 (0.72-0.94)	0.76 (0.72-0.94)	0.79 (0.74-0.95)	0.79 (0.74-0.95)
Perimural signal intensity	0.95 (0.85-1.00)	0.95 (0.85-1.00)	0.95 (0.84-1.00)	0.95 (0.84-1.00)
Ascending colon				
Mural thickness	0.85 (0.74-1.00)	0.85 (0.74-1.00)	0.85 (0.80-1.00)	0.85 (0.80-1.00)
Mural signal intensity	0.85 (0.70-1.00)	0.85 (0.70-1.00)	0.85 (0.70-1.00)	0.85 (0.70-1.00)
Perimural signal intensity	0.79 (0.57-1.00)	0.79 (0.57-1.00)	0.79 (0.57-1.00)	0.79 (0.57-1.00)

Data in parenthesis are 95% confidence interval.
CR = conventional reconstruction, DLR = deep-learning based reconstruction, MBH = multiple-breath-hold, SBH = single-breath-hold

and MBH schemes ($p > 0.001$).

ACQUISITION TIME

The mean acquisition time of the MBH images was 53.19 s (SD: 3.16, range: 49–65 s), and that of the SBH images was 16.29 s (SD: 0.99, range: 13–20 s).

DISCUSSION

Our study demonstrated that applying DLR in SSFSE T2-weighted images in MRE improves image quality compared with that of conventionally reconstructed images. The SBH technique has advantages over the MBH technique, such as reducing misalignments (MBH vs. SBH: 52% vs. 3.3%, $p < 0.001$) and scan time (MBH vs. SBH: 53 s vs. 16 s). SBH-DLR showed an equivalent image quality in terms of the overall quality, artifacts, and sharpness of bowel and vessel structures compared to that of MBH-CR, which is the current standard of care. Moreover, the inter-reader and inter-sequence agreements were excellent for all the three parameters used to evaluate the inflammation caused by Crohn's disease, suggesting that the diagnostic performance was not affected.

A slice misalignment between BHs was more frequently observed in the MBH images than in the SBH images. Our results showed that the misalignment was more statistically significant in the MBH group. The coverage of the entire scan range in the SBH technique could eliminate this spatial mismatch as it prevents the unintentional skipping of anatomical details or lesions caused by a slice misalignment. Because DLR was not designed to correct this misalignment, the CR and corresponding DLR images showed no difference.

The SBH sequence can be acquired in approximately 16 s, while the MBH sequence can be acquired in 53 s over three BHs. Considering the total scan time of MRE, which is approxi-

https://doi.org/10.3348/jksr.2023.0008

Table 5. Inter-Sequence Agreement on Inflammatory Lesions

	MBH-DLR vs. MBH-CR		MBH-DLR vs. SBH-DLR		MBH-DLR vs. SBH-CR		MBH-CR vs. SBH-DLR		MBH-CR vs. SBH-CR		SBH-DLR vs. SBH-CR	
	Reader 1	Reader 2	Reader 1	Reader 2	Reader 1	Reader 2	Reader 1	Reader 2	Reader 1	Reader 2	Reader 1	Reader 2
Ileum												
Mural thickness	1.00 (1.00–1.00)	1.00 (1.00–1.00)	0.99 (0.96–1.00)	0.98 (0.95–1.00)	0.99 (0.96–1.00)	1.00 (1.00–1.00)	0.99 (0.96–1.00)	0.98 (0.95–1.00)	0.99 (0.96–1.00)	1.00 (1.00–1.00)	1.00 (1.00–1.00)	0.98 (0.95–1.00)
Mural signal intensity	1.00 (1.00–1.00)	1.00 (1.00–1.00)	0.96 (0.91–1.00)	0.96 (0.90–1.00)	0.96 (0.91–1.00)	0.96 (0.90–1.00)	0.96 (0.91–1.00)	0.96 (0.90–1.00)	0.96 (0.91–1.00)	0.96 (0.90–1.00)	1.00 (1.00–1.00)	1.00 (1.00–1.00)
Perimural signal intensity	1.00 (1.00–1.00)	1.00 (1.00–1.00)	1.00 (1.00–1.00)	1.00 (1.00–1.00)	1.00 (1.00–1.00)	1.00 (1.00–1.00)	1.00 (1.00–1.00)	1.00 (1.00–1.00)	1.00 (1.00–1.00)	1.00 (1.00–1.00)	1.00 (1.00–1.00)	1.00 (1.00–1.00)
Terminal ileum												
Mural thickness	1.00 (1.00–1.00)	1.00 (1.00–1.00)	0.97 (0.94–1.00)	0.96 (0.92–1.00)	0.97 (0.94–1.00)	0.96 (0.92–1.00)	0.97 (0.94–1.00)	0.96 (0.92–1.00)	0.97 (0.94–1.00)	0.96 (0.92–1.00)	1.00 (1.00–1.00)	1.00 (1.00–1.00)
Mural signal intensity	1.00 (1.00–1.00)	1.00 (1.00–1.00)	1.00 (1.00–1.00)	1.00 (1.00–1.00)	1.00 (1.00–1.00)	0.96 (0.92–1.00)	1.00 (1.00–1.00)	1.00 (1.00–1.00)	1.00 (1.00–1.00)	0.98 (0.95–1.00)	1.00 (1.00–1.00)	0.98 (0.95–1.00)
Perimural signal intensity	1.00 (1.00–1.00)	1.00 (1.00–1.00)	0.95 (0.84–1.00)	0.95 (0.85–1.00)	0.95 (0.84–1.00)	0.95 (0.85–1.00)	0.95 (0.84–1.00)	0.95 (0.85–1.00)	0.95 (0.84–1.00)	0.95 (0.85–1.00)	1.00 (1.00–1.00)	1.00 (1.00–1.00)
Ascending colon												
Mural thickness	1.00 (1.00–1.00)	1.00 (1.00–1.00)	1.00 (1.00–1.00)	0.97 (0.91–1.00)	1.00 (1.00–1.00)	0.97 (0.91–1.00)	1.00 (1.00–1.00)	0.97 (0.91–1.00)	1.00 (1.00–1.00)	0.97 (0.91–1.00)	1.00 (1.00–1.00)	1.00 (1.00–1.00)
Mural signal intensity	1.00 (1.00–1.00)	1.00 (1.00–1.00)	1.00 (1.00–1.00)	1.00 (1.00–1.00)	1.00 (1.00–1.00)	1.00 (1.00–1.00)	1.00 (1.00–1.00)	1.00 (1.00–1.00)	1.00 (1.00–1.00)	1.00 (1.00–1.00)	1.00 (1.00–1.00)	1.00 (1.00–1.00)
Perimural signal intensity	1.00 (1.00–1.00)	1.00 (1.00–1.00)	1.00 (1.00–1.00)	1.00 (1.00–1.00)	1.00 (1.00–1.00)	1.00 (1.00–1.00)	1.00 (1.00–1.00)	1.00 (1.00–1.00)	1.00 (1.00–1.00)	1.00 (1.00–1.00)	1.00 (1.00–1.00)	1.00 (1.00–1.00)

Data in parenthesis are 95% confidence interval.
CR = conventional reconstruction, DLR = deep-learning based reconstruction, MBH = multiple-breath-hold, SBH = single-breath-hold

JOURNAL of THE KOREAN SOCIETY of RADIOLOGY

mately 40–45 min, the time saved was minimal. However, because patients ingest more than 1000 mL of oral contrast, endure abdominal symptoms and urgency during the scan, and repeat breath-holding, they get exhausted easily. Thus, even the smallest duration reduction can help them to better tolerate the exam and cooperate. In addition, SBH imaging could help in reducing motion artifacts caused by gross bowel movement between BHs, which might hinder the anatomic details of the bowel.

The main contributor to the low scores in the overall image artifact category was the multiple fine linear artifacts that appeared throughout the entire image, particularly in the SBH image sets. They were identified as free-induction decay (FID) artifacts or fine-line artifacts. FID artifacts are more prominent when applying a VFA because of the overlapping of incompletely crushed FID signals from a radiofrequency refocusing pulse, which manifest as ripples or ring-like artifacts (20, 21). Although the use of DLR reduces artifacts, it is specifically designed to reduce the truncation ones (9); therefore, it cannot eliminate FID artifacts completely. Nevertheless, these artifacts were observed less frequently in the SBH-DLR images than in the SBH-CR images, resulting in an improved image quality and reduced overall artifacts.

Motion-related signal loss, which is usually associated with cardiac motion, is another common artifact typically observed in the left upper quadrant of the abdomen, especially when a VFA is applied. The reduced refocusing FA and long refocusing pathways allow the accumulation of phase shifts from motion, resulting in a bulk area of signal loss (10, 22). The SBH images, in which a VFA was applied, had a tendency toward signal loss in the left upper margin of the image compared with the MBH images that maintained a constant refocusing FA. The corresponding DLR images showed no significant improvement in signal loss. However, most signal losses were confined to the left liver and did not affect the diagnostic capability to detect bowel inflammation in most cases.

Mural or perimural T2 signal intensity and bowel wall thickening indicate active inflammation in patients with Crohn's disease (15). Previous studies have shown that the a VFA application can improve image contrast by reducing the effective rate of T2 relaxation and decreasing image blurring through the stabilization of the signal amplitude through the echo train compared with SSFSE, in which a constant refocusing FA is used (10, 12, 23). Nevertheless, if the T2 signal intensity or bowel wall thickness varies according to the sequences imaged, it may be difficult to diagnose inflammation. In our study, the agreements of the inflammatory parameters were high between the readers and between the sequences, suggesting that the differences in the refocusing FA and the image reconstruction methods do not affect the evaluation of bowel wall inflammation.

Our study had a few limitations. First, it had a retrospective design and was performed at a single institution. Second, the quality difference between the images was sufficient to estimate the sequence and reconstruction methods; therefore, the reviewers were not completely blinded, which might have been a source of potential bias.

In conclusion, the SBH images with DLR demonstrated nearly an equivalent image quality without changes in interpretation when evaluating bowel inflammation compared to the MBH images with CR. Furthermore, this sequence can be acquired in less than half of the scan time without exhausting multiple BHs and reducing slice misalignment. Considering these characteristics, SBH-SSFSE imaging with DLR may be considered an alternative to the

conventional methods.

Author Contributions

Conceptualization, L.Y., L.J.; data curation, all authors; formal analysis, P.E.J., L.Y.; investigation, P.E.J., L.Y.; methodology, P.E.J., L.J.; project administration, L.Y.; supervision, L.Y.; visualization, all authors; writing—original draft, P.E.J.; and writing—review & editing, P.E.J., L.Y.

Conflicts of Interest

The authors have no potential conflicts of interest to disclose.

Funding

None

REFERENCES

1. Grand DJ, Guglielmo FF, Al-Hawary MM. MR enterography in Crohn's disease: current consensus on optimal imaging technique and future advances from the SAR Crohn's disease-focused panel. *Abdom Imaging* 2015;40:953-964
2. Rimola J, Ordás I, Rodriguez S, García-Bosch O, Aceituno M, Llach J, et al. Magnetic resonance imaging for evaluation of Crohn's disease: validation of parameters of severity and quantitative index of activity. *Inflamm Bowel Dis* 2011;17:1759-1768
3. Rimola J, Rodriguez S, García-Bosch O, Ordás I, Ayala E, Aceituno M, et al. Magnetic resonance for assessment of disease activity and severity in ileocolonic Crohn's disease. *Gut* 2009;58:1113-1120
4. Ziech ML, Bipat S, Roelofs JJ, Nio CY, Mearadji B, van Doorn S, et al. Retrospective comparison of magnetic resonance imaging features and histopathology in Crohn's disease patients. *Eur J Radiol* 2011;80:e299-e305
5. Siddiki HA, Fidler JL, Fletcher JG, Burton SS, Huprich JE, Hough DM, et al. Prospective comparison of state-of-the-art MR enterography and CT enterography in small-bowel Crohn's disease. *AJR Am J Roentgenol* 2009;193:113-121
6. Lee MG, Jeong YK, Kim JC, Kang EM, Kim PN, Auh YH, et al. Fast T2-weighted liver MR imaging: comparison among breath-hold turbo-spin-echo, HASTE, and inversion recovery (IR) HASTE sequences. *Abdom Imaging* 2000;25:93-99
7. Nakayama Y, Yamashita Y, Matsuno Y, Tang Y, Namimoto T, Kadota M, et al. Fast breath-hold T2-weighted MRI of the kidney by means of half-Fourier single-shot turbo spin echo: comparison with high resolution turbo spin echo sequence. *J Comput Assist Tomogr* 2001;25:55-60
8. Makowski MR, Wiethoff AJ, Jansen CH, Uribe S, Parish V, Schuster A, et al. Single breath-hold assessment of cardiac function using an accelerated 3D single breath-hold acquisition technique--comparison of an intravascular and extravascular contrast agent. *J Cardiovasc Magn Reson* 2012;14:53
9. Sheng RF, Zheng LY, Jin KP, Sun W, Liao S, Zeng MS, et al. Single-breath-hold T2WI liver MRI with deep learning-based reconstruction: a clinical feasibility study in comparison to conventional multi-breath-hold T2WI liver MRI. *Magn Reson Imaging* 2021;81:75-81
10. Loening AM, Saranathan M, Ruangwattanapaisarn N, Litwiller DV, Shimakawa A, Vasanawala SS. Increased speed and image quality in single-shot fast spin echo imaging via variable refocusing flip angles. *J Magn Reson Imaging* 2015;42:1747-1758
11. Jabarkheel R, Tong E, Lee EH, Cullen TM, Yousaf U, Loening AM, et al. Variable refocusing flip angle single-shot imaging for sedation-free fast brain MRI. *AJNR Am J Neuroradiol* 2020;41:1256-1262
12. Loening AM, Litwiller DV, Saranathan M, Vasanawala SS. Increased speed and image quality for pelvic single-shot fast spin-echo imaging with variable refocusing flip angles and full-Fourier acquisition. *Radiology* 2017;282:561-568
13. Wang S, Xiao T, Liu Q, Zheng H. Deep learning for fast MR imaging: a review for learning reconstruction from incomplete k-space data. *Biomed Signal Process Control* 2021;68:102579
14. Lebel RM. Performance characterization of a novel deep learning-based MR image reconstruction pipeline. arXiv [Preprint]. 2020 [cited 2022 June 17]. Available at: https://doi.org/10.48550/arXiv.2008.06559

15. Kim J, Seo N, Bae H, Kang EA, Kim E, Chung YE, et al. Comparison of sensitivity encoding (SENSE) and compressed sensing-SENSE for contrast-enhanced T1-weighted imaging in patients with Crohn disease undergoing MR enterography. *AJR Am J Roentgenol* 2022;218:678-686
16. Kaltenbach B, Bucher AM, Wichmann JL, Nickel D, Polkowski C, Hammerstingl R, et al. Dynamic liver magnetic resonance imaging in free-breathing: feasibility of a Cartesian T1-weighted acquisition technique with compressed sensing and additional self-navigation signal for hard-gated and motion-resolved reconstruction. *Invest Radiol* 2017;52:708-714
17. Steward MJ, Punwani S, Proctor I, Adjei-Gyamfi Y, Chatterjee F, Bloom S, et al. Non-perforating small bowel Crohn's disease assessed by MRI enterography: derivation and histopathological validation of an MR-based activity index. *Eur J Radiol* 2012;81:2080-2088
18. Pimpalkhute VA, Page R, Kothari A, Bhurchandi KM, Kamble VM. Digital image noise estimation using DWT coefficients. *IEEE Trans Image Process* 2021;30:1962-1972
19. Dietrich O, Raya JG, Reeder SB, Reiser MF, Schoenberg SO. Measurement of signal-to-noise ratios in MR images: influence of multichannel coils, parallel imaging, and reconstruction filters. *J Magn Reson Imaging* 2007;26:375-385
20. Mugler JP 3rd. Optimized three-dimensional fast-spin-echo MRI. *J Magn Reson Imaging* 2014;39:745-767
21. Bernstein MA, Huston J 3rd, Ward HA. Imaging artifacts at 3.0T. *J Magn Reson Imaging* 2006;24:735-746
22. Ruangwattanapaisarn N, Loening AM, Saranathan M, Litwiller DV, Vasanawala SS. Faster pediatric 3-T abdominal magnetic resonance imaging: comparison between conventional and variable refocusing flip-angle single-shot fast spin-echo sequences. *Pediatr Radiol* 2015;45:847-854
23. Hicks RM, Loening AM, Ohliger MA, Vasanawala SS, Hope TA. Variable refocusing flip angle single-shot fast spin echo imaging of liver lesions: increased speed and lesion contrast. *Abdom Radiol (NY)* 2018;43:593-599

J Korean Soc Radiol 2023;84(6):1309-1323

JOURNAL of THE KOREAN SOCIETY of RADIOLOGY

크론병에서 자기공명영상 장운동기록의 단일호흡 단발 고속 스핀 에코기법: 딥러닝 기반 재구성의 영향

박언주[1] · 이예다운[1*] · 이준성[2]

목적 크론병 환자의 자기공명영상 장운동기록(MR enterography; 이하 MRE)에서 단발 고속 스핀 에코기법(single-shot fast spin-echo; 이하 SSFSE)을 이용한 단일호흡영상(single-breath-hold; 이하 SBH)과 다호흡영상(multiple-breath-hold; 이하 MBH)을 딥러닝 기반 재구성(deep-learning based reconstruction; 이하 DLR)의 유무에 따라 네 개의 영상에서 품질을 비교했다.

대상과 방법 이 연구는 후향적 연구로서, 크론병으로 MRE를 시행한 61명의 환자가 포함되었다. SBH와 MBH SSFSE 영상에서 각각 DLR과 고식적 재구성(conventional reconstruction; 이하 CR)을 시행한 영상을 획득했다. 두 명의 영상의학과 전문의가 네 가지 영상을 분석하여 전반적인 영상의 품질, 인공물, 선명도와 움직임 관련 신호 손실에 대하여 각각 5점 척도를 이용해 점수를 부여했다. 회장과 말단 회장, 결장에서 염증을 시사하는 세 가지 소견을 평가했다. 각 영상에 대해서 공간적 불일치 여부를 확인했고, 네 가지 영상에서 각각 다른 두 위치에서 신호 대 잡음비(signal-to-noise ratio; 이하 SNR)를 계산했다.

결과 SBH SSFSE 영상에서 DLR을 적용한 경우 CR보다 영상의 품질, 인공물, 선명도가 통계학적으로 유의하게 개선되었다. 네 가지 영상 중 SBH-DLR 영상에서 SNR이 가장 높게 나타났다($p < 0.001$). 염증 소견에 대한 판독자 간 일치율은 좋음에서 매우 좋음으로 나타났고($\kappa = 0.76–0.95$) 시퀀스 간 일치율은 매우 좋음으로 측정되었다($\kappa = 0.92–0.94$). 공간적 불일치는 SBH 영상보다 MBH 영상에서 통계학적으로 유의하게 빈도가 높았다($p < 0.001$).

결론 SBH-DLR 영상은 MBH-CR 영상과 비교했을 때 동등한 영상 품질과 성능을 보여주었다. 또한, MBH 영상에 비해 절반 이하의 시간과 단일 호흡만으로 영상을 획득할 수 있으며 공간 불일치를 줄일 수 있는 대체제로 사용할 수 있다.

[1]인제대학교 의과대학 해운대백병원 영상의학과,
[2]GE 헬스케어코리아